Preclinical Characterization of Allogeneic CAR γδ T Cell Therapy for Prostate Cancer Targeting a Novel Dimeric Epitope on PSMA

Nitya S. Ramadoss, Elizabeth Speltz, Tonya Capillo, Erika Meaddough, Natalia Friedland, Katherine Wang, Jonathan Wong, Alexander G. Teague, Aruna Azameera, Smitha Rao Yelaguli Gundurao, Ramandeep Kaur, Morgan Smith-Boeck, Michael Salum, Demetrio Cardenas, Yvan Chanthery, Shon Green, Marissa Herrman, Kevin P. Nishimoto, Blake T. Aftab, Arun Bhat
Adicet Bio, Inc. Redwood City, CA 94065

INTRODUCTION

PSMA is a transmembrane glycosylated homodimer overexpressed in >80% of prostate cancers and demonstrates increased expression in advanced stages of the disease. Clinically, autologous anti-PSMA αβ CAR T cells have shown signs of activity but have limited therapeutic index. We are developing an allogeneic γδ CAR T platform associated with activation-induced cytokine profiles that may decrease CRS-associated toxicities. Compared to αβ T cells and other innate cells, γδ T cells are capable of multifunctional innate and adaptive targeting and infiltrate into prostate tumor-associated tissues. Here, we characterized γδ T cells engineered with CARs developed from a set of novel scFvs and identified and characterized lead candidates with unique epitopes targeting homodimeric PSMA. Formation of homodimeric PSMA is necessary for enzymatic function and formation of this homodimer introduces conformational epitopes that are potentially more distinct from linear epitopes and potentially reduce off-targeting of PSMA-like proteins.

METHODS

Phage panning was used to identify anti-PSMA scFv sequences, which were reformatted into IgGs and characterized for binding to both cells expressing endogenous PSMA and recombinant PSMA. Binders with favorable profiles were reformatted into CARs in VH-VL and VL-VH orientations and transduced into Vδ1 T cells, a primarily tissue-resident subset, activated from healthy donor PBMCs. We identified lead CARs based on anti-tumor efficacy both *in vitro* in coculture assays and *in vivo* in tumor xenograft models and compared their activity to Vδ1 CAR T cells transduced with a clinically validated benchmark, J591. Epitope mapping of binders in the lead CARs was performed using a funnel of molecular assays including dot blots, competition assays, and cross-linking mass spectrometry (XL-MS).

Anti-PSMA antibodies obtained from phage display bind specifically to PSMA with varying affinities

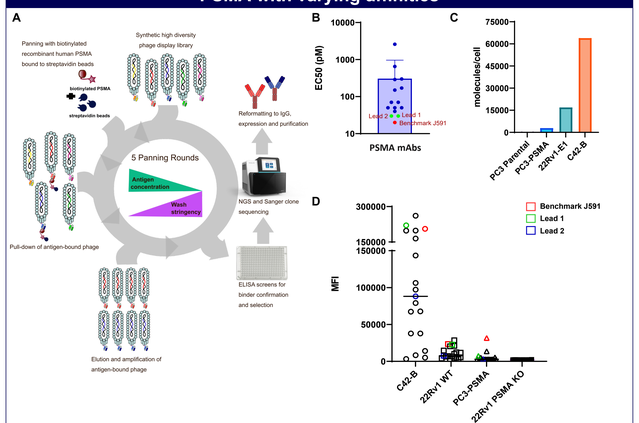

Figure 1. (A) Overview of panning process to identify anti-PSMA binders. **(B)** Reformatted IgGs (mAbs) from (A) were characterized for binding properties on recombinant protein using ELISA. Range of EC50 values are shown for all mAbs tested **(C)** PSMA expression levels were determined in PCa cell lines **(D)** mAbs were additionally tested for binding to PCa cells with high, medium and low PSMA expression. Specificity of mAbs were also assessed using the 22Rv1-PSMA KO cell line, which has no PSMA expression.

Lead anti-PSMA antibodies preferentially bind to native antigen

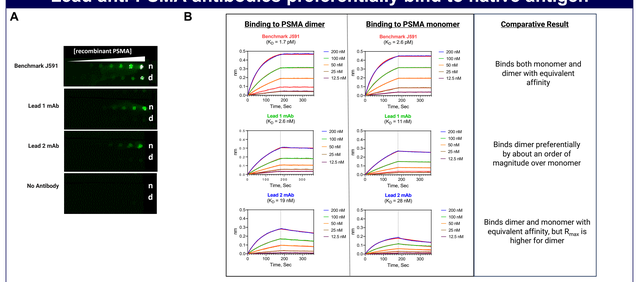

Figure 2. (A) Dot blot showing binding of benchmark J591 and two lead anti-PSMA antibodies to recombinant human PSMA protein in its native form ('n') or denatured form ('d'). **(B)** Bio-layer interferometry sensograms showing binding of benchmark J591 and two lead antibodies to various concentrations of recombinant human PSMA protein equilibrated in 2M NaCl without EDTA (predominantly dimer) and with 2mM EDTA (predominantly monomer). Fits of the sensograms are in red. Table on right details interpretation of the data.

Lead anti-PSMA antibodies bind to membrane-distal, conformational epitopes distinct from that of J591, a well-known benchmark

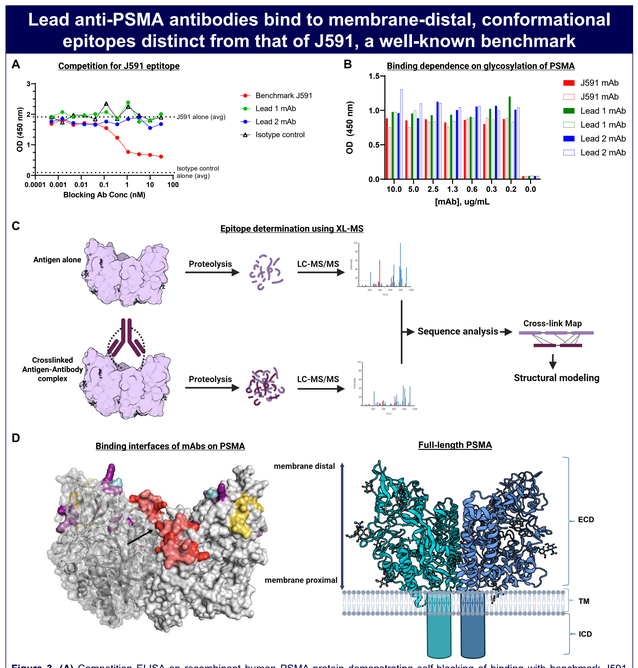

Figure 3. (A) Competition ELISA on recombinant human PSMA protein demonstrating self-blocking of binding with benchmark J591 (blue squares) and lack of blocking of J591 binding by other lead antibodies (red circles, yellow triangles). **(B)** Binding of benchmark J591 and anti-PSMA antibodies to native (filled bars) and deglycosylated (open bars) PSMA protein **(C)** Schematic describing the process of conformational epitope mapping using cross-linking mass spectrometry (XL-MS) **(D)** Binding interfaces of lead anti-PSMA antibodies displayed on a surface representation of the homodimeric x-ray crystal structure of the PSMA extracellular domain (PDB ID: 1Z8L) in red (lead 1) and purple (lead 2), in comparison to that of J591 (yellow). Predicted glycosylation site near epitope of lead 2 is shown in teal. Black arrow indicates one of the helices involved in homodimer formation, which is the enzymatically active form of the target. Cartoon on right panel shows overall architecture of full-length PSMA homodimer.

Anti-PSMA CAR-expressing Jurkat cells show target-specific activation and low tonicity

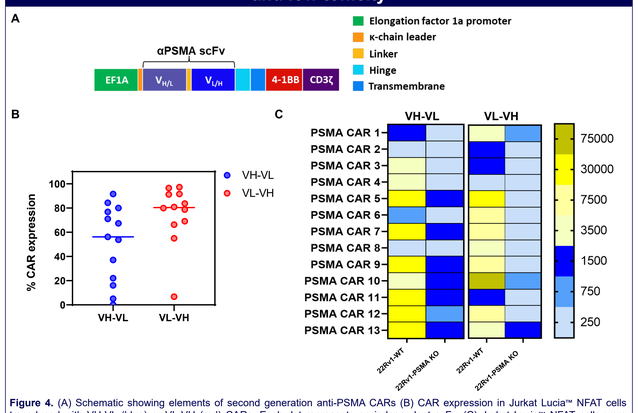

Figure 4. (A) Schematic showing elements of second generation anti-PSMA CARs (B) CAR expression in Jurkat Lucia™ NFAT cells transduced with VH-VL (blue) or VL-VH (red) CARs. Each dot represents an independent scFv, (C) Jurkat Lucia™ NFAT cells were transduced with gammaretrovirus to express CARs in VH-VL and VL-VH orientations, then co-cultured with 22Rv1-WT cells and 22Rv1-PSMA KO cells to assess antigen-specific activation. Supernatants from co-cultures were incubated with luciferase and resultant luminescence was plotted as NFAT activity in heatmap format, with each row representing an independent scFv.

Anti-PSMA CAR Vδ1 T cells expand robustly in multiple donors and are efficacious against PCa cell lines *in vitro*

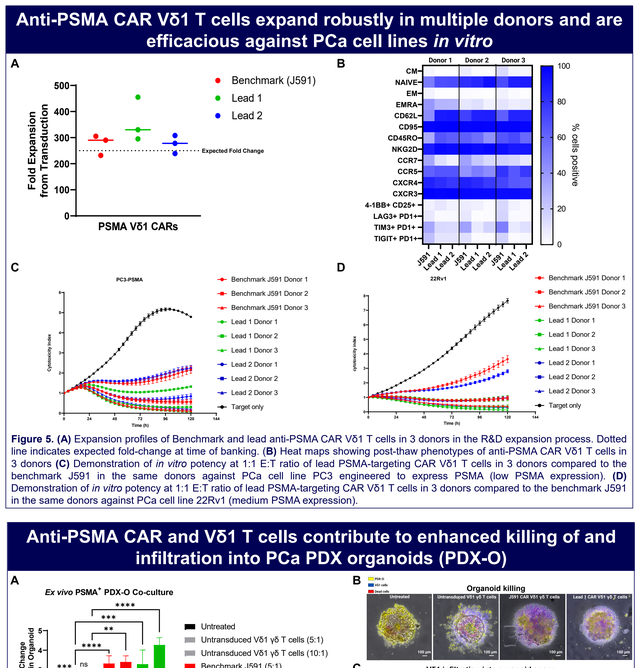

Figure 5. (A) Expansion profiles of Benchmark and lead anti-PSMA CAR Vδ1 T cells in 3 donors in the R&D expansion process. Dotted line indicates expected fold-change at time of banking. **(B)** Heat maps showing post-thaw phenotypes of anti-PSMA CAR Vδ1 T cells in 3 donors **(C)** Demonstration of *in vitro* potency at 1:1 E:T ratio of lead PSMA-targeting CAR Vδ1 T cells in 3 donors compared to the benchmark J591 in the same donors against PCa cell line PC3 engineered to express PSMA (low PSMA expression). **(D)** Demonstration of *in vitro* potency at 1:1 E:T ratio of lead PSMA-targeting CAR Vδ1 T cells in 3 donors compared to the benchmark J591 in the same donors against PCa cell line 22Rv1 (medium PSMA expression).

Anti-PSMA CAR and Vδ1 T cells contribute to enhanced killing of and infiltration into PCa PDX organoids (PDX-O)

Figure 6. (A) Patient-derived xenograft (PDX) fragments were stained with CellTrace Yellow and seeded in 96w plates. Upon organoid formation, Vδ1 T cells were stained with CellTrace Violet and added to the organoid cultures at 10:1 and 5:1 E:T ratios. Bar graphs show dead cell quantification within organoid structures after 4 days of co-culture as a fold-change from untreated organoids. **(B)** Representative images showing organoid killing by Vδ1 T cells and anti-PSMA CAR Vδ1 T cells after 4 days of co-culture. **(C)** Representative images from showing the Vδ1 T cell channel alone (E:T = 10:1). White arrow indicates un-infiltrated organoid space.

Anti-PSMA CAR Vδ1 T cells expanded in multiple donors show robust tumor control *in vivo* in a challenging PCa Xenograft model

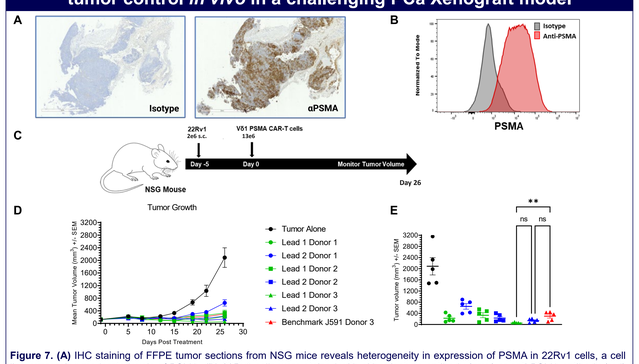

Figure 7. (A) IHC staining of FFPE tumor sections from NSG mice reveals heterogeneity in expression of PSMA in 22Rv1 cells, a cell line expressing moderate levels of PSMA. **(B)** 22Rv1 cells were stained with either isotype antibody (grey) or anti-PSMA antibody (red) and analyzed by flow cytometry. **(C)** Schematic outlines the study design for demonstration of *in vivo* potency in a 22Rv1 PCa xenograft model with PSMA-targeting Vδ1 CAR T cells expanded in 3 donors. Graphs detail tumor volumes determined for the entire study duration **(D)** as well as statistical comparison of treatment groups relative to the benchmark at study termination **(E)**.

Anti-PSMA CAR Vδ1 T cells armored with dnTGFβRII show enhanced tumor control in the presence of TGFβ1

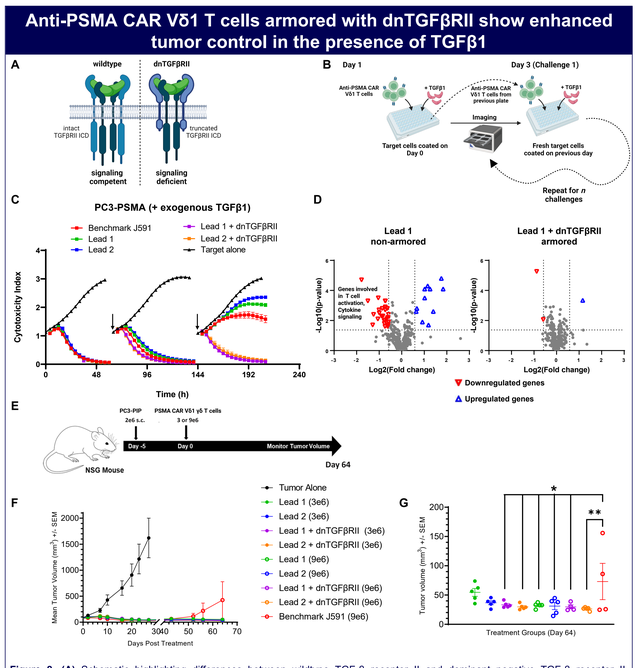

Figure 8. (A) Schematic highlighting differences between wildtype TGF-β receptor II and dominant negative TGF-β receptor II (dnTGFβRII) **(B)** Schematic describing *in vitro* target re-challenge assay to assess cytotoxic ability of armored anti-PSMA CAR Vδ1 T cells in the presence of exogenous TGFβ1 **(C)** Anti-PSMA CAR Vδ1 T cells, with or without armoring were co-cultured with PC3-PSMA target cells at an E:T ratio of 3:1 in the presence of TGFβ1 for 3 days before re-challenging with fresh PC3-PSMA target cells in the presence of TGFβ1. Cytotoxicity indices are plotted over time. Black arrows indicate points of rechallenge **(D)** Nanostring analysis of Lead 1 CAR Vδ1 T cells without (left panel) and with dnTGFβRII armoring (right panel) stimulated with recombinant human PSMA protein in the presence and absence of TGFβ1 reveals downregulation of genes associated with T cell activation and cytokine signaling for CAR without armor **(E)** Schematic outlines the study design for demonstration of *in vivo* potency in a PC3-PIP PCa xenograft model with PSMA-targeting Vδ1 CAR-T cells with or without the dnTGFβRII, tested at two doses. **(F)** Graph details tumor volumes determined for the entire study duration **(G)** Statistical comparison of treatment groups relative to the benchmark at study termination.

SUMMARY & CONCLUSIONS

- Vδ1 T cells modified to express PSMA CARs from *de novo* discovery were screened and characterized.
- Novel binders in lead PSMA CARs target conformational, membrane-distal epitopes that are distinct from the predicted linear epitope for J591, a well-known clinical benchmark.
- Binding to unique, conformational epitopes may reduce off-targeting of PSMA-like proteins.
- Potent tumor growth inhibition by lead PSMA CAR Vδ1 T cells, in addition to intrinsic Vδ1 targeting, was observed in heterogeneous and uniform PCa tumor xenograft models, as well as in 3D PDX organoids.
- A functional advantage with armoring (dnTGFβRII) was demonstrated for the anti-PSMA CAR Vδ1 T cells.
- In summary, these preclinical data support further development of an armored allogeneic γδ CAR T cell therapy for prostate cancer.

References

1. Schulke, N. et al. The homodimer of prostate-specific membrane antigen is a functional target for cancer therapy. PNAS 100 (22) 12590-95 (2003). https://doi.org/10.1073/pnas.1735443100
2. Davis, M. et al. Crystal structure of prostate-specific membrane antigen, a tumor marker and peptidase. PNAS 102(17):5981-6 (2005). https://doi.org/10.1073/pnas.0502101102
3. Yu C, Huang L. Cross-Linking Mass Spectrometry: An Emerging Technology for Interactomics and Structural Biology. Anal Chem. 90(1):144-165 (2018). https://doi.org/10.1021/acs.analchem.7b04431
4. Kaushik G, Verma B, Wesa A. (88) Development of a 3D organoid autologous TIL co-culture platform for high throughput immuno-oncology studies. JITC (2020).https://doi.org/10.1136/jitc-2020-SITC2020.0088
5. Narayan, V., Barber-Rotenberg, J.S., Jung, IY. et al. PSMA-targeting TGFβ-insensitive armored CAR T cells in metastatic castration-resistant prostate cancer: a phase 1 trial. Nat Med 28, 724–734 (2022). https://doi.org/10.1038/s41591-022-01726-1
6. Neelapu, S. S., Stevens, D.A., Hamadani, M., et al. A Phase I Study of ADI-001: Anti-CD20 CAR-Engineered Allogeneic Gamma Delta 1 T cells in Adults with B-cell Malignancies. Blood 140 (Supplement 1): 4617-1619 (2022). https://doi.org/10.1182/blood-2022-157400
7. Sebestyen, Z., Prinz, I., Dechanet-Merville, J. et al. Translating gammadelta T cells and their receptors into cancer cell therapies. Nat Rev Drug Discov 19(3):169-184 (2020). https://doi.org/10.1038/s41573-019-0038-z
8. Multiple schematics and cartoons in this poster were created with BioRender.com